Available online at www.sciencedirect.com

Journal of Catalysis 224 (2004) 340–346

JOURNAL OF CATALYSIS

www.elsevier.com/locate/jcat

Decomposition of CCl_3F over vanadium oxides and $[MgV_xO_y]MgO$ shell/core-like particles

Igor N. Martyanov and Kenneth J. Klabunde *

Department of Chemistry, Kansas State University, 111 Willard Hall, Manhattan, KS 66506, USA

Received 13 March 2003; revised 12 September 2003; accepted 16 February 2004

Available online 21 April 2004

Abstract

Decomposition of gaseous CCl_3F over in-house-prepared V_2O_3 (HP-V_2O_3), commercial V_2O_3, VO_2, V_2O_5, a mechanical mixture of the HP-V_2O_3/Aerogel-prepared MgO (AP-MgO), and $[MgV_xO_y]MgO$ shell/core-like particles at 280 °C has been investigated with FTIR spectroscopy. The reaction of CCl_3F with the HP-V_2O_3 proceeds vigorously. Intermediate compounds including CCl_4, CCl_2F_2, CCl_2O, and final gaseous products $CClF_3$, CO_2 were detected. No chloride/fluoride was found on the sample surface, suggesting the formation of volatile vanadium–halogen products as well. Vanadium–chloride product was found to react with the surface of the bare AP-MgO leading to deposition of vanadium–chloride species. Activities of VO_2 and V_2O_3 were found to be qualitatively similar to the HP-V_2O_3. The reaction of CCl_3F with V_2O_5 proceeds much slower, with only CCl_2O and CO_2 gaseous products observed. Activation of the AP-MgO with vanadium-containing species leads to formation of $[MgV_xO_y]MgO$ shell/core-like particles. The MgO crystalline phase was the only one detected in the $[MgV_xO_y]MgO$ samples. In the reaction with CCl_3F, the $[MgV_xO_y]MgO$ samples retain some properties characteristic for the bare AP-MgO (presence of an induction period for $V/Mg = 1$ mol%, lower activity toward CCl_4 than toward CCl_2F_2 for $V/Mg = 1$, 10 mol%), and some properties characteristic for the HP-V_2O_3/AP-MgO mechanical mixture (accumulation of chlorine but no fluorine on the $[MgV_xO_y]MgO$, $V/Mg = 10$ mol% sample surface).

© 2004 Elsevier Inc. All rights reserved.

Keywords: MgO; V_2O_3; V_2O_5; CCl_3F; Magnesium oxide; Vanadium oxide; Freon; Decomposition; Nanoparticles; Catalysis

1. Introduction

About a decade ago alkaline-earth metal oxides were found to be active in numerous destructive adsorption processes including but not limited to detoxification of chlorine- [1–5] and phosphorous- [6,7] containing organic compounds as well as flue [8] gases. The properties of these oxides have been thoroughly studied [9–13] and the advantages of their nanoparticulate form have been well documented.

Recently, nanoparticulate Aerogel-prepared MgO (AP-MgO) was found to be active [14,15] in the destruction of ozone-damaging [16,17] CCl_2F_2 and CCl_3F gases. Interestingly, these reactions begin very slowly but drastically accelerate over time. Accumulation of halogens on the AP-MgO surface followed by formation of a $MgO_xCl_yF_z$ intimate mixture was suggested to be the reason for the reaction acceleration.

The positive catalytic influence of transition metal oxide additives on AP-MgO performance with respect to CCl_3F destructive adsorption could be expected from earlier studies. Indeed, coverage of alkaline-earth particles with a shell of transition metal oxides considerably improved AP-MgO and CaO sorption abilities [1,9]. In the case of CCl_4 destruction over AP-MgO, the effectiveness for reaction promotion increased in the following order [1]:

$$\mathrm{Sc} < \mathrm{none} < \mathrm{Cr} < \mathrm{Ni} < \mathrm{Cu} < \mathrm{Ti} < \mathrm{Zn} < \mathrm{Fe} < \mathrm{Co} < \mathrm{Mn} < \mathrm{V}.$$

In this regard investigation of the interaction of vanadium-activated AP-MgO with CCl_3F could be of particular interest for a number of reasons. First, among all transition metals tested, the vanadium additive allowed the highest activity to be achieved. Second, upon the reaction of the vanadium additive with CCl_3F, formation of relatively mobile and consequently more easily detected vanadium halogen-containing

---

[*] Corresponding author. Fax: (785) 532 6666.
E-mail address: kenjk@ksu.edu (K.J. Klabunde).

0021-9517/$ – see front matter © 2004 Elsevier Inc. All rights reserved.
doi:10.1016/j.jcat.2004.02.026

species can be expected. Third, a difference in the chemistry of chlorine- and fluorine-containing compounds could be explored, which may help in elucidating a reaction mechanism. Having this in mind, studies of the reactivity of vanadium oxides and vanadium-activated AP-MgO shell/core-like particles toward trichlorofluoromethane decomposition were carried out herein and compared with activity of the bare AP-MgO.

2. Experimental

2.1. Reagents and materials

CCl_3F, CF_2Cl_2 of "pure" grade, CCl_4, V_2O_3, VO_2, V_2O_5, $[(CH_3)_2CHO]_3VO$, and CO_2 (Aldrich), toluene, and methanol (Fisher) were used as received.

2.1.1. AP-MgO preparation

Preparation of Aerogel-prepared MgO (AP-MgO) has been described earlier [9]. In short this includes formation of $Mg(OCH_3)_2$ via reaction of Mg with CH_3OH, dilution of $Mg(OCH_3)_2$ with toluene, formation of $Mg(OH)_2$ with water addition, supercritical drying of $Mg(OH)_2$ suspension, and conversion of $Mg(OH)_2$ into AP-MgO via heat treatment under dynamic vacuum at 500 °C overnight.

2.1.2. In-house-prepared vanadium oxide (HP-V_2O_3) preparation procedure

Initially two mixtures were prepared. The first one was obtained via addition of 1.1 mL of water to 20 mL of toluene kept under continuous ultrasound sonication (Fisher Scientific). The second one was obtained via dissolution of 4.72 mL of $[(CH_3)_2CHO]_3VO$ into 20 mL of toluene. About 30 min after sonication was started the second mixture was slowly added to the first one. The resultant suspension was kept under continuous sonication for 60 min in an open beaker. Later the toluene was removed under dynamic vacuum (10^{-2} Torr) at room temperature overnight followed by high-temperature vacuum treatment at 300 °C for 30 min and at 500 °C for 1 h.

2.1.3. Mechanical HP-V_2O_3/AP-MgO mixture preparation

Preliminary estimated quantities of the HP-V_2O_3 and the AP-MgO were carefully mixed to produce a composition with a ratio of V to Mg moles equal to 0.1 ($V/Mg =$ 10 mol%).

2.1.4. $[MgV_xO_y]$MgO shell/core-like particles preparation procedure

Initially two mixtures were prepared. The first mixture was made by addition of 0.2 g of AP-MgO to 5 mL of toluene kept under continuous ultrasound sonication. The second one contained 12 or 118 µL of $[(CH_3)_2CHO]_3VO$ dissolved in 5 mL of toluene. The next steps were similar to those used for HP-V_2O_3 preparation. With 12 or 118 µL the samples contained on average $V/Mg = 1$ or 10% by molar percentage. Though no water was added, the amount of H_2O and OH groups held on the AP-MgO surface was sufficient to provide complete $[(CH_3)_2CHO]_3VO$ hydrolysis.

2.2. Sample characterization

A scanning electron microscope (SEM, Hitachi Science System) was used for obtaining sample images and determination of their elemental composition. The samples were pressed into a tungsten mesh and necessarily exposed to air prior to introduction in the SEM vacuum chamber. Energy dispersive X-ray analysis (EDXA) with 20 keV electron acceleration voltage allowed determination of surface elemental composition of samples. An element was considered to be present on a sample surface if its concentration exceeded the ca. 0.5 mol% detection limit.

Surface area of the samples was derived with the multipoint BET method from nitrogen adsorption isotherms measured at 77 K on a NOVA-1200 (Quantachrome Corporation). Before surface area measurements, samples were additionally degassed at 500 °C under dynamic vacuum (10^{-2} Torr) for 1 h.

A Sintag diffractometer working in a step mode (0.02° step, 1 s/step accumulation time) was employed for determining powder X-ray diffractograms (XRD) of the samples. All recordings were carried out in open air with no additional sample pretreatment.

2.3. Kinetic experiments

All experiments were carried out in a stainless-steel IR-cell [18] (350 mL) connected to the vacuum line, power supply, temperature controller, and equipped with KBr crystal windows. An FTIR spectrometer (Mattson company) was used to record IR spectra at 1-min intervals with 1 cm^{-1} resolution.

2.3.1. Experiments with vanadium oxides (HP-V_2O_3, and commercial V_2O_3, VO_2, V_2O_5), mechanical HP-V_2O_3/AP-MgO mixture, and $[MgV_xO_y]$MgO shell/core-like particles

About 0.1 g of sample was pressed into tungsten (or in the case of V_2O_5, VO_2, and V_2O_3 into molybdenum) mesh, inserted into the IR cell followed by sample pretreatment under dynamic vacuum ca. 10^{-5} Torr at 500 °C for 1 h. Later, the sample was cooled to 280 °C (if not stated otherwise), 1.5 Torr of CCl_3F was introduced, the cell was closed, and the spectra recording procedure was started. No oxygen was fed in the IR cell. The IR beam passed only through the gas phase; thus, changes in the gas phase were followed.

2.3.2. Experiments with the sample consisting of separated spots of the AP-MgO and the HP-V_2O_3

Preliminary estimated amounts of the HP-V_2O_3 and the AP-MgO were pressed into a tungsten mesh as separate spots in different locations on the grid. Total amounts of each compound, their ratio, and further procedures were similar to those used in the kinetic experiments with the mechanical HP-V_2O_3/AP-MgO mixture.

2.3.3. *Quantitative measurements*

Current CCl_3F, CCl_4, and CCl_2F_2 concentrations were calculated from areas under characteristic peaks of IR spectra followed by comparison with corresponding calibration curves. In the case of $CClF_3$, and CCl_2O, no calibration curves were available, so their concentrations are shown in arbitrary units (A.U.). Due to the difficulties of taking into account CO_2 localized outside the IR cell, CO_2 kinetic curves are also shown in A.U. In most cases superimposition of absorption peaks originating from different compounds could be neglected, although the measured value of the CCl_3F peak at 846 cm^{-1} was corrected for the presence of CCl_2O.

3. Results and discussion

3.1. *Vanadium oxides*

XRD patterns of different vanadium oxides used in the present study are shown in Fig. 1. Comparison of the XRD pattern of the in-house-prepared vanadium oxide with commercially available V_2O_3 revealed their structural similarities so that in-house-prepared vanadium oxide was designated as HP-V_2O_3. Surface areas of the samples derived from nitrogen adsorption measurements were HP-V_2O_3 (5 m^2/g), V_2O_3 (1.6 m^2/g), VO_2 (2.7 m^2/g), and V_2O_5 (4.0 m^2/g).

Fig. 2 presents the gas-phase IR spectra recorded during the first 10 min of the reaction of CCl_3F with HP-V_2O_3 at $T = 280\,°C$. Absorption bands of the reaction products pertaining to CCl_3F, CCl_2F_2, CCl_4, CCl_2O, and CO_2 are readily noticeable. Two absorption bands around 1830 cm^{-1} attributed to phosgene are followed by a weak unidentified doublet at ca. 1880 cm^{-1}. It is worth noting that the similar unidentified product was observed during reaction of chlorobenzene with V_2O_5 [19], suggesting that this compound does not contain fluorine. Since the spectrum of this unknown compound (at least in the region near 1880 cm^{-1}) is similar to phosgene (with some shift to higher wavenumbers) and the concentrations of phosgene and the unknown product correlate with each other it can be suggested that the unidentified product is a result of CCl_2O interaction with a vanadium-containing gas.

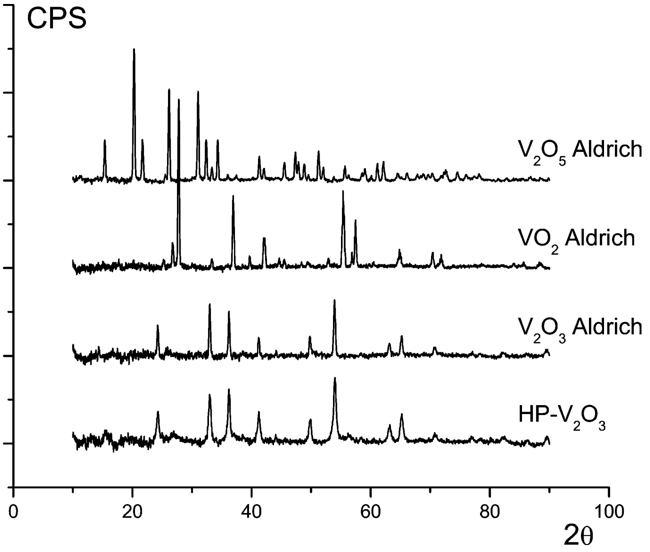

Fig. 1. XRD patterns of various vanadium oxide powders tested in the reaction with CCl_3F. Vertical scale is presented in counts per second (CPS) with base lines deliberately shifted for clarity.

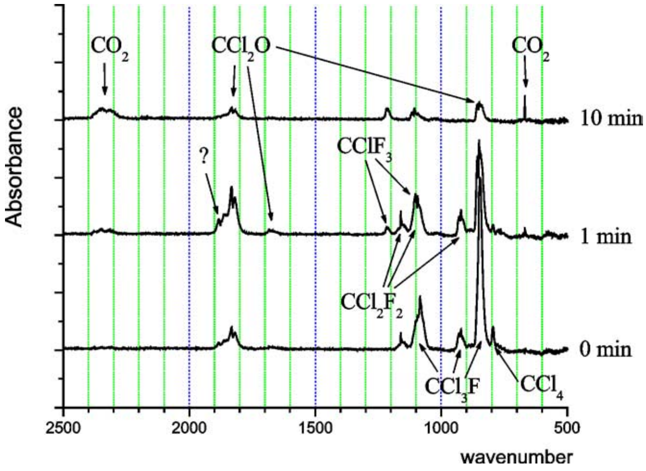

Fig. 2. Gas-phase FTIR spectra recorded in situ at various times elapsed after CCl_3F was brought into contact with the HP-V_2O_3 maintained at $T = 280\,°C$.

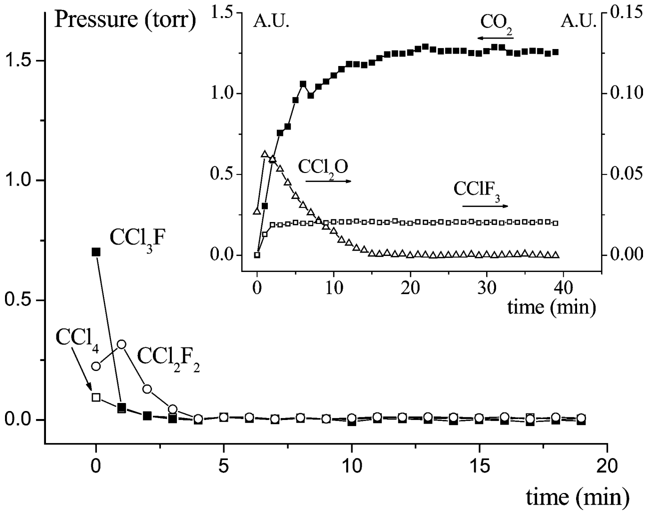

Fig. 3. Time evolution of different gaseous compound concentrations after introduction of CCl_3F to the HP-V_2O_3 maintained at $T = 280\,°C$. The course of the reaction was followed by FTIR.

Fig. 3 shows the evolution of CCl_3F, CCl_4, CCl_2F_2, $CClF_3$, CCl_2O, and CO_2 concentrations with time. Just 4 min is enough to eliminate CCl_3F, CCl_4, and CCl_2F_2

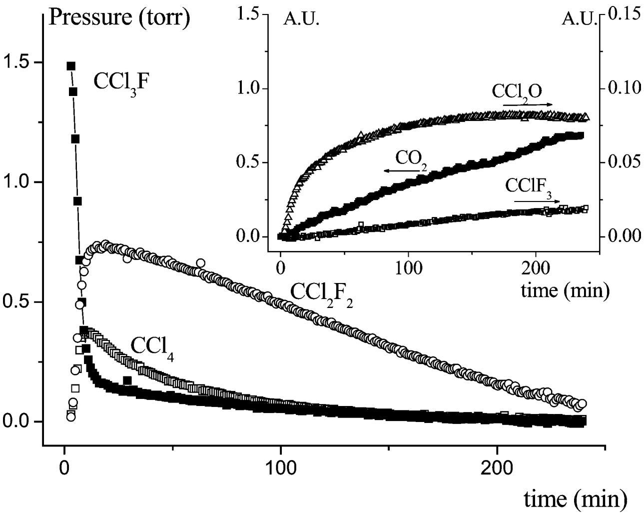

Fig. 4. Time evolution of different gaseous compound concentrations after introduction of CCl_3F to the HP-V_2O_3 maintained at $T = 180\,^\circ C$.

Table 1
The presence of Mg, V, Cl, F, and O elements detected at sample surfaces by EDX analysis

	Mg V Cl F O	
	Before reaction with CCl_3F	After reaction with CCl_3F
HP-V_2O_3	− + − − +	− + − − +
Spot of AP-MgO (with HP-V_2O_3 spot situated near by)	+ − − − +	+ + + − +
Shell/core [MgV_xO_y]MgO $V/Mg = 10\%$	+ + − − +	+ + + − +

The "+" refers to a positive identification, "−" refers to the situation when the concentration of an element was below 0.5 at% detection limit.

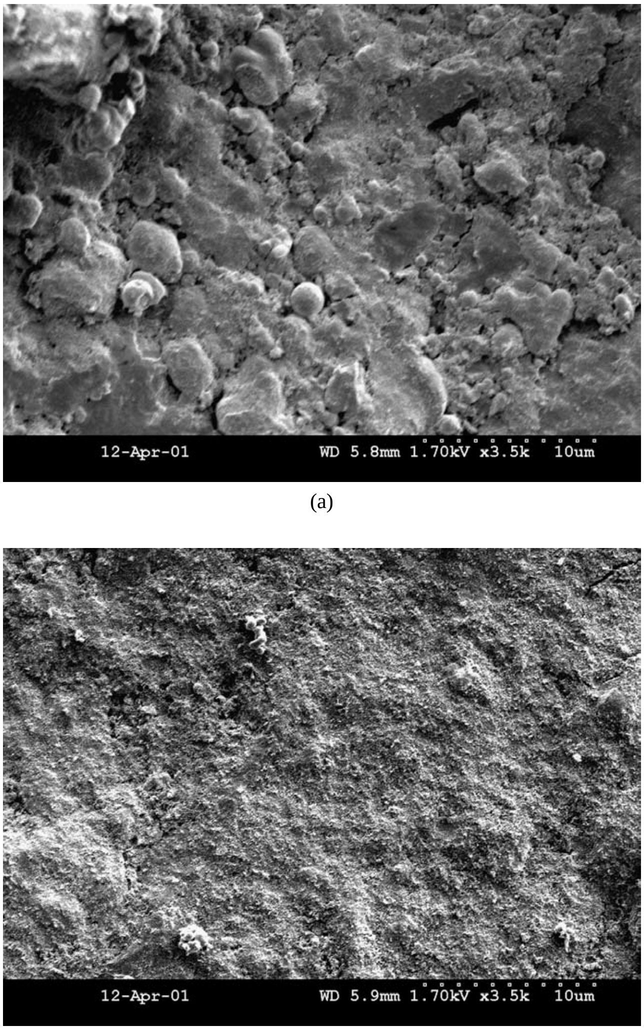

(a)

(b)

Fig. 5. SEM images of the HP-V_2O_3 before (a) and after (b) the reaction.

gases. Conversion of CCl_2O into CO_2 proceeds later. CO_2, $CClF_3$, and traces of HCl were the only final products detected.

To see the beginning of the process in more detail, the same reaction was carried out at 180 °C (Fig. 4) instead of 280 °C. Even at this lower temperature, still no induction period typical for the bare AP-MgO [15] was observed. Initially, decomposition of CCl_3F leads to equal amounts of CCl_4 and CCl_2F_2. Soon, however, the CCl_4 and CCl_2F_2 concentrations reach maximal values and begin to fall with CCl_4 disappearing faster than CCl_2F_2.

Elemental analysis of the HP-V_2O_3 samples before and after the reaction revealed no presence of even trace amounts of chlorine or fluorine moieties (Table 1), whereas SEM images gave evidence of surface etching (Fig. 5). These findings indicate that vanadium–chlorine/fluorine species forming during the reaction are volatile at 280 °C and leave the surface of the sample.

To gain some information about the influence of vanadium oxidation state on sample reactivity, experiments with commercially available V_2O_3, VO_2, and V_2O_5 were carried out. The V_2O_3 and VO_2 samples demonstrated activity qualitatively similar to HP-V_2O_3. However, the behavior of V_2O_5 was completely different. Though the surface area of V_2O_5 was higher than that of commercial V_2O_3, V_2O_5 was much less active toward CCl_3F with no CCl_4, CCl_2F_2, and $CClF_3$ formed (Fig. 6).

Activity of V_2O_5 [19–22] and various $V_xO_y^+$ positively charged clusters [23,24] participating in the reaction with CCl_4 were studied earlier. In the case of V_2O_5, formation of CO_2, CCl_2O, and $VOCl_3$ was observed. It was found that while CO_2 concentration gradually increased and CCl_2O passed through a maximum, the $VOCl_3$ concentration reached a limiting value and did not change later on as the reaction progressed [21].

The experiments with vanadium oxide clusters are of special interest since the reactivity of vanadium in different oxidation states was explored. In particular, it was found that the clusters containing vanadium in low oxidation states were considerably more active and reacted in a way different from the clusters where the oxidation state of vanadium was +5.

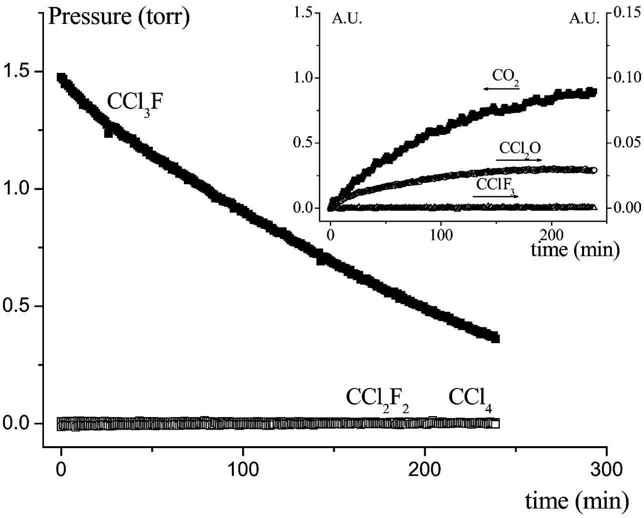

Fig. 6. Time evolution of different compound concentrations after exposure of the commercial V_2O_5 maintained at $T = 280\,°C$ to CCl_3F. The reaction conditions are the same as in Fig. 2.

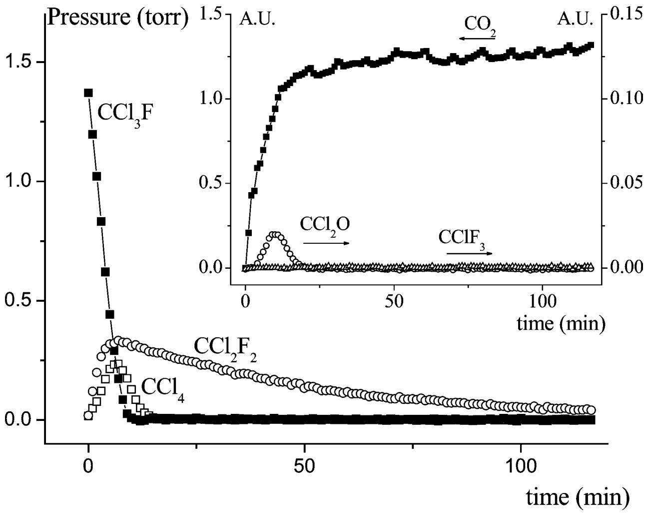

Fig. 7. Time evolution of different compound concentrations after mechanical HP-V_2O/AP-MgO mixture (V/Mg = 10 mol%) was brought into contact with CCl_3F; $T = 280\,°C$.

For example, the $V_3O_6{}^+$ cluster (formal vanadium oxidation state is $+4\frac{1}{3}$) reacted with abstraction of chlorine atom,

$$V_3O_6{}^+ + CCl_4 \rightarrow V_3O_6Cl^+ + CCl_3, \quad (1)$$

whereas the $V_3O_7{}^+$ cluster containing vanadium atoms in the +5 oxidation state was much less active and reacted with phosgene formation,

$$V_3O_7{}^+ + CCl_4 \rightarrow V_3O_6Cl_2{}^+ + CCl_2O. \quad (2)$$

Note that cluster $V_3O_7{}^+$ cannot accept a chlorine atom because it cannot provide electrons for an additional vanadium–chlorine bond. Instead, that cluster prefers to exchange oxygen for two chlorine atoms. In this respect the clusters containing vanadium in an oxidation state lower than +5 have certain advantages since they can easily provide electrons for initiating bond formation.

These results seem to be in good agreement with the present work. In accordance with the literature data [23], the reaction of CCl_3F with bulk V_2O_5 proceeds slowly with CCl_2O to be the only detectable intermediate product. The samples containing vanadium in +3 oxidation state are considerably more active with CCl_4, CCl_2F_2, and CCl_2O as intermediate species.

3.2. Mechanical HP-V_2O_3/AP-MgO mixture

The course of the reaction of CCl_3F with a mechanical mixture of HP-V_2O_3/AP-MgO having V/Mg = 10% molar ratio and kept at 280 °C is shown in Fig. 7. As this sample contained a lower amount of the HP-V_2O_3, the reaction progressed slower than with the pure HP-V_2O_3 (Fig. 3). At the same time the evolution of different compound concentrations was quite similar to the HP-V_2O_3 alone with exception that no $CClF_3$ was observed. From these considerations we conclude that in the early stages of reaction, HP-V_2O_3 is the major active component of the HP-V_2O_3/AP-MgO mechanical mixture.

To trace vanadium movements, an experiment with separated spots (different locations on the grid) of the AP-MgO and the HP-V_2O_3 was carried out. Elemental analysis revealed (Table 1) that some vanadium as well as chlorine but no fluorine was deposited on the AP-MgO. This is probably due to the higher reactivity of vanadium–chlorine compounds, which would be volatile and move to the surface of the MgO, exchanging chlorine for oxygen at reactive sites. Vanadium–fluorine compounds would be less volatile (compare, for example, boiling points of VOF_3 (480 °C) with analogous $VOCl_3$ (126.7 °C)) [25] and perhaps more thermodynamically stable and therefore would be less likely to interact with the MgO surface. Since the atomic ratio of chlorine to vanadium deposited was $Cl/V = 3.2 \pm 0.4$, VCl_3 might be considered as a possible volatile vanadium–chlorine-containing compound involved in the reaction.

3.3. [MgV_xO_y]MgO shell/core-like particles

Activation of the AP-MgO with the vanadium additive results in a substantial surface area decrease: AP-MgO (530 m^2/g), [MgV_xO_y]MgO (V/Mg = 1 mol%) (359 m^2/g), [MgV_xO_y]MgO (V/Mg = 10 mol%) (110 m^2/g). Since deposition of the vanadium compound on the AP-MgO was done in a way similar to the preparation of HP-V_2O_3, formation of a V_2O_3 phase on the top of the AP-MgO might be expected. However, as it is evident from the XRD data presented in Fig. 8, no new crystalline phase forms upon heating of the AP-MgO with the vanadium species. This result is not unusual in view of earlier studies where vanadium oxides were found to react with MgO at elevated temperatures forming numerous compounds [26]. Having this in mind and due to the higher vanadium concentration at the

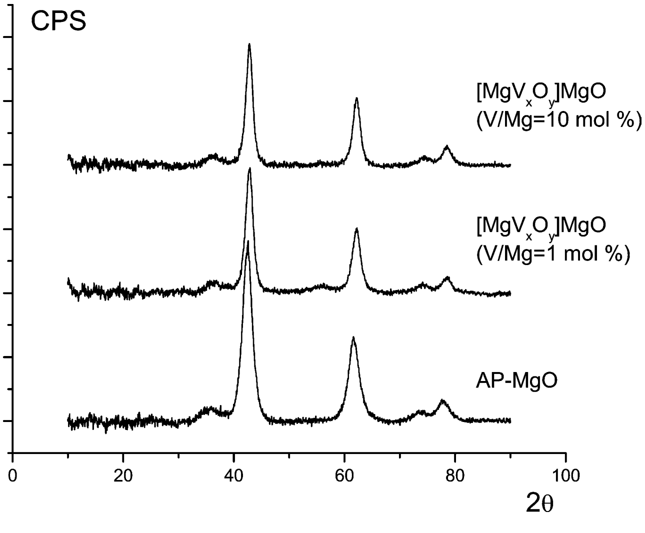

Fig. 8. XRD patterns of the AP-MgO and the [MgV$_x$O$_y$]MgO shell/core-like samples with different vanadium contents.

MgO surface, vanadium-activated (heat treated) magnesium oxide particles are denoted herein as [MgV$_x$O$_y$]MgO.

The formation of an intimate mixture of the AP-MgO and vanadium oxide results in the appearance of a new compound, [MgV$_x$O$_y$]MgO (Figs. 9 and 10), with some properties similar to and some properties different from the properties of the bare AP-MgO, HP-V_2O_3, or their mechanical mixture. Indeed, [MgV$_x$O$_y$]MgO (V/Mg = 1 mol%) demonstrates the presence of an induction period typical for the AP-MgO [15], but not for the HP-V_2O_3. Interaction of CCl_3F with the [MgV$_x$O$_y$]MgO results in the appearance of CCl_4, and CCl_2F_2 (Fig. 9). Although these intermediates are typical for both the AP-MgO [15] and the HP-V_2O_3 (Figs. 3 and 4), the lesser stability of CCl_2F_2 as compared to CCl_4 makes the [MgV$_x$O$_y$]MgO sample resemble the AP-MgO rather than the HP-V_2O_3. The ability for the accumulation of halogens is yet another way to stress the similarities and the differences in the properties of the [MgV$_x$O$_y$]MgO and the AP-MgO, HP-V_2O_3, as well as the AP-MgO/HP-V_2O_3 mechanical mixture. As can be seen from the results of Table 1, the [MgV$_x$O$_y$]MgO demonstrates an ability to accumulate chorine but no fluorine, whereas the AP-MgO accumulates both chorine and fluorine [15]. The AP-MgO/HP-V_2O_3 mechanical mixture accumulates chlorine but no fluorine and none of the halogens deposit on the HP-V_2O_3 surface.

Based on the experimental data and the consideration given above, the following conclusions regarding the process of decomposition of CCl_3F over [MgV$_x$O$_y$]MgO core/shell-like particles can be drawn. Addition of vanadium moieties to the shell of AP-MgO particles leads to substantial activation of the AP-MgO. However, in the case of small amounts of vanadium (V/Mg = 1 mol%), the role of vanadium as an activator is mainly seen in its influence on the induction period of the reaction. Indeed, in comparison with the bare AP-MgO, introduction of such a small amount of vanadium shortens the induction period of the reaction but does not eliminate it entirely. Thus, by analogy with the bare AP-MgO [15] it is reasonable to suggest that the presence of the vanadium additive accelerates accumulation of halogens (mainly chlorine) on the surface of MgO and is followed by formation of a MgV$_x$O$_y$Cl$_z$ intimate mixture. The MgV$_x$O$_y$Cl$_z$ mixture is more active than the initial MgV$_x$O$_y$ so that acceleration of the reaction takes place.

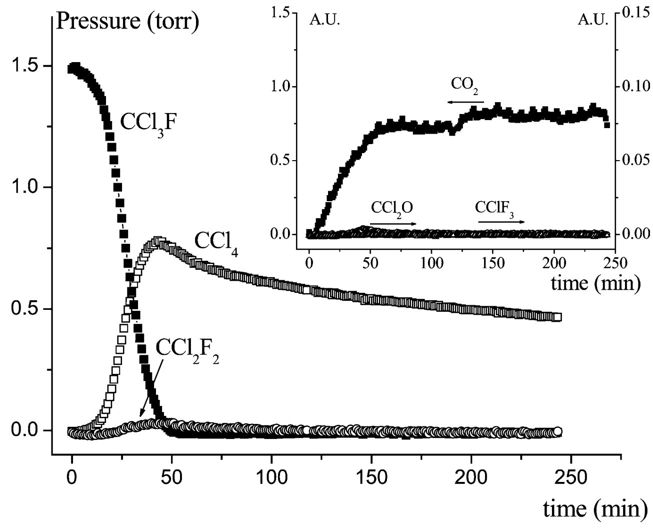

Fig. 9. Time evolution of different gaseous compound concentrations after [MgV$_x$O$_y$]MgO shell/core-like sample (V/Mg = 1 mol%) was brought into contact with CCl_3F; $T = 280\,^{\circ}C$.

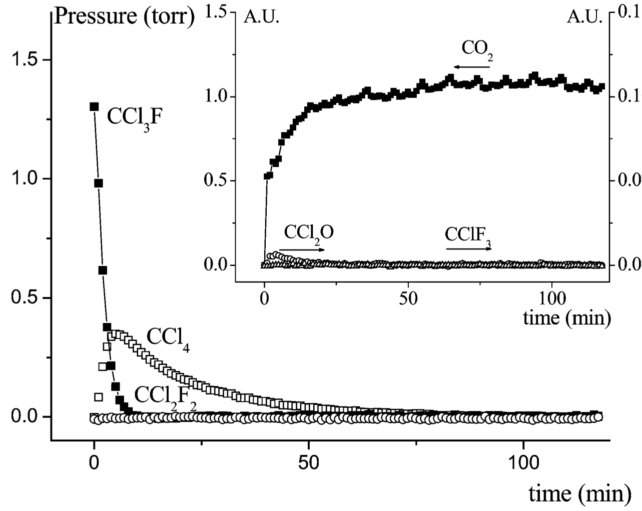

Fig. 10. Time evolution of different compound concentrations after [MgV$_x$O$_y$]MgO shell/core-like sample (V/Mg = 10 mol%) was brought into contact with CCl_3F; $T = 280\,^{\circ}C$.

Overall, the following processes (not balanced) are thought to be responsible for the observed behavior of [MgV$_x$O$_y$]MgO samples. First, the reaction of the vanadium containing part of the shell, [MgV$_x$O$_y$], with CCl_3F leads to chlorine accumulation:

$$[\mathrm{MgV}_x\mathrm{O}_y]\mathrm{MgO} + \mathrm{CCl_3F} \rightarrow [\mathrm{MgV}_x\mathrm{O}_y][\mathrm{MgV}_x\mathrm{O}_y\mathrm{Cl}_z]\mathrm{MgO} + \mathrm{VF}_y + \mathrm{CO_2}. \qquad (3)$$

Since the $[MgV_xO_yCl_z]$ is more active than $[MgV_xO_y]$, the observed reaction acceleration takes place. Higher activity of $[MgV_xO_y]$ with respect to the bare MgO [15] explains the shorter induction period of the reaction. Later, $[MgV_xO_yCl_z]$ may react with CCl_3F giving CCl_4:

$$[MgV_xO_y][MgV_xO_yCl_z]MgO + CCl_3F \rightarrow [MgV_xO_y][MgV_xO_yCl_z]MgO + VF_y + CCl_4. \quad (4)$$

Fast reaction of $[MgV_xO_yCl_z]$ with CCl_3F and CCl_4 should lead to progressive substitution of surface oxygen by chorine until complete oxygen exhaustion. At this point, vanadium may leave the surface in the forms of volatile VCl_x as in the processes used for extraction of vanadium from ores [27]:

$$[MgV_xO_y][MgV_xO_yCl_z]MgO + CCl_3F/CCl_4 \rightarrow [MgV_xO_y][MgCl_2]MgO + VCl_x + VF_y + CO_2. \quad (5)$$

In the presence of bare MgO, VCl_x reacts with it creating active $[MgV_xO_yCl_z]$:

$$[MgV_xO_y][MgCl_2]MgO + VCl_x \rightarrow [MgV_xO_y][MgCl_2][MgV_xO_yCl_z]MgO. \quad (6)$$

In excess of CCl_3F, conversion of $[MgV_xO_y]MgO$ into MgF_2 as the most thermodynamically stable magnesium compounds and volatile vanadium–halogens can be expected:

$$[MgV_xO_y]MgO + CCl_3F \rightarrow MgF_2 + VCl_x + VF_y + CCl_4 + CO_2. \quad (7)$$

4. Conclusions

In-house prepared V_2O_3 (HP-V_2O_3) was found to be the most active in the decomposition of CCl_3F as compared with the commercial V_2O_5, VO_2, and V_2O_3. The HP-V_2O_3 is consumed in the reaction so that besides CO_2 and some $CClF_3$, the reaction products include vanadium–halogen species that leave the surface of the HP-V_2O_3 under the reaction conditions studied.

Formation of the volatile vanadium–halogen species followed by their recapture by bare MgO is thought to be the reason behind the catalytic influence of vanadium additives on the performance of the AP-MgO in the destructive absorption of CCl_3F. As a result, the $[MgV_xO_y]MgO$ samples demonstrate higher activities and shorter induction periods as compared to the bare AP-MgO. As the reaction proceeds, the activity of the $[MgV_xO_y]MgO$ with a low vanadium loading level additionally enhances due to the accumulation of chorine.

Acknowledgment

The support of the Army Research Office (DAAD 19-01-10619) is acknowledged with gratitude.

References

[1] Y. Jiang, S. Decker, C. Mohs, K.J. Klabunde, J. Catal. 180 (1998) 24.
[2] O. Koper, I. Lagadic, K.J. Klabunde, Chem. Mater. 9 (1997) 838.
[3] O. Koper, E.A. Wovchko, J.A. Glass Jr., J.T. Yates Jr., K.J. Klabunde, Langmuir 11 (1995) 2054.
[4] Y.-X. Li, H. Li, K.J. Klabunde, Environ. Sci. Technol. 28 (1994) 1248.
[5] O. Koper, Y.-X. Li, K.J. Klabunde, Chem. Mater. 5 (1993) 500.
[6] Y.-X. Li, K.J. Klabunde, Langmuir 7 (1991) 1388.
[7] Y.-X. Li, O. Koper, M. Atteya, K.J. Klabunde, Chem. Mater. 4 (1992) 323.
[8] J.V. Stark, D.G. Park, I. Lagadic, K.J. Klabunde, Chem. Mater. 8 (1996) 1905.
[9] S. Utamapanya, K.J. Klabunde, J.R. Schlup, Chem. Mater. 3 (1991) 175.
[10] K.J. Klabunde, J. Stark, O. Koper, C. Mohs, D.G. Park, S. Decker, Y. Jiang, I. Lagadic, D. Zhang, J. Phys. Chem. 100 (1996) 12142.
[11] R.M. Morris, K.J. Klabunde, Inorg. Chem. 22 (1983) 682.
[12] H. Itoh, S. Utamapanya, J.V. Stark, K.J. Klabunde, J.R. Schlup, Chem. Mater. 5 (1993) 71.
[13] O. Koper, I. Lagadic, A. Volodin, K.J. Klabunde, Chem. Mater. 9 (1997) 2468.
[14] I.V. Mishakov, A.F. Bedilo, V.V. Chesnokov, S.V. Filimonova, I.N. Martyanov, K.J. Klabunde, A.M. Volodin, V.N. Parmon, in preparation.
[15] I.N. Martyanov, K.J. Klabunde, in preparation.
[16] M.J. Molina, F.S. Rowland, Nature 249 (1974) 810.
[17] G.J. Wolff, in: J.I. Kroschwitz, M. Howe-Grant (Eds.), Encyclopedia of Chemical Technology, vol. 1, Wiley, New York, 1994, p. 715.
[18] P. Basu, T.H. Ballinger, J.T. Yates Jr., Rev. Sci. Instrum. 59 (1988) 1321.
[19] S.B. Geyer, L.R. Brock, J.W. Keister, T.C. DeVore, Electrochem. Soc. Proc. 97 (39) (1997) 298.
[20] G. Mink, I. Bertoti, T. Szekely, React. Kinet. Catal. Lett. 27 (1) (1985) 33.
[21] G. Mink, I. Bertoti, C. Battistoni, T. Szekely, React. Kinet. Catal. Lett. 27 (1) (1985) 39.
[22] G. Mink, I. Bertoti, I.S. Pap, T. Szekely, C. Battistoni, E. Karmazsin, Thermochim. Acta 85 (1985) 83.
[23] R.C. Bell, K.A. Zemski, A.W. Castleman Jr., J. Phys. Chem. 103 (1999) 1585.
[24] R.C. Bell, K.A. Zemski, A.W. Castleman Jr., J. Phys. Chem. 103 (1999) 2992.
[25] R.C. Weast (Ed.), Handbook of Chemistry and Physics, fifty fourth ed., CRC Press, Cleveland, 1974.
[26] H. Oshima, J. Am. Ceram. Soc. 63 (1980) 504.
[27] S.A. Amirova, V.V. Pechkovskii, R. Kurmaev, Kh. Tsvetn. Metal. 36 (1963) 57.